INCORRECT CONTACT OF SCREW SURFACES AND NUMERICAL SOLUTION OF THE LEAKAGE FLOW THROUGH THE ARISEN GAP

Jan Vimmr*, Jaromír Švígler*

The article deals with the incorrect contact of screw surfaces which create tooth faces of screw-type machine rotors and is concerned about the turbulent computation of a gas leakage through a two-dimensional model of an undesirable gap caused by the incorrect contact of rotor teeth screw surfaces. The incorrect contact of rotor teeth screw surfaces, considered in this study, is caused by a parallel displacement of the male rotor axis. The problem of the leakage flow through the two-dimensional model of the undesirable gap is solved as a non-stationary turbulent compressible Newtonian fluid flow with ideal gas properties. The turbulent flow is assumed to be statistically steady and the mathematical model is described by the non-linear conservative system of the compressible Favre-averaged Navier-Stokes equations. Its numerical solution is performed using the cell-centred finite volume formulation of the explicit two-step TVD MacCormack scheme which is proposed by Causon and is defined on a structured quadrilateral grid. To simulate the turbulence effects the algebraic Baldwin-Lomax turbulence model is implemented into the developed numerical code.

Key words: *screw-type machine, incorrect contact of rotor teeth, gas leakage, compressible flow, turbulence, Favre-averaged Navier-Stokes equations, finite volume method, TVD MacCormack scheme*

1. Introduction

Mathematical modelling of transonic flow of viscous compressible fluids in very narrow channels is one of the very topical and demanding problems of internal aerodynamics today. Screw-type machines, i.e. screw compressors or expanders that create in combination with compressors the screw engines, represent one of many examples. The most important part of a screw compressor, Fig. 1 (left), is its work space. It is created by screw surfaces of both rotor teeth, Fig. 1 (right), and by the inner surface of the compressor housing. The screw compressor work space has a complex geometry [10], which volume makes smaller during the rotors motion. That causes the compression of the fluid. The work space chambers are separated by three main types of clearance gaps – frontal gaps at axial ends of rotors, gaps between rotors themselves and gaps between rotors and compressor housing. The processes, which take place in work space chambers and especially in clearance gaps on their boundaries, have a significant influence on the screw-type machine performance. The knowledge of the gas leakage in clearance gaps is essential to make reasonable estimates for the mass flow rate and to define the loss of the medium. From this point of view the investigation of the leakage flow through the clearance gaps in screw-type machines is necessary. The leakage flow can

* Ing. J. Vimmr, Ph.D., doc. Ing. J. Švígler, CSc., Department of Mechanics, Faculty of Applied Sciences, University of West Bohemia in Pilsen, Univerzitní 22, 306 14 Plzeň, Czech Republic

be reasonably modelled by computational fluid dynamics for so called dry compressors, Fig. 1 (left), where no multiphase flow occurs.

The leakage flow in the clearance gaps is studied by many screw compressor engineers, e.g. [7], [8] or [9]. In [7] and [8] many experimental and numerical simulations of compressible viscous fluid flow through a two-dimensional model of the male rotor-housing gap (the sealing gap between the head of the male rotor tooth and machine housing) in a screw compressor for various pressure ratios are presented. All of these numerical simulations were only performed by available commercial software package Fluent using various turbulence models and the rotary motion of the male rotor was not involved in the computations. In [14] and [15], the turbulent computation of the gas leakage in a two-dimensional model of the 100 μm wide male rotor-housing gap was performed using the numerical code developed by the author. The situation for the typical pressure ratio $p_{\mathrm{inlet}}/p_{\mathrm{outlet}} = 2$ between neighbouring work space chambers was studied. The static pressure distribution in the two-dimensional model of the male rotor-housing gap computed in [15] was qualitatively compared with the pressure measurements published in [7].

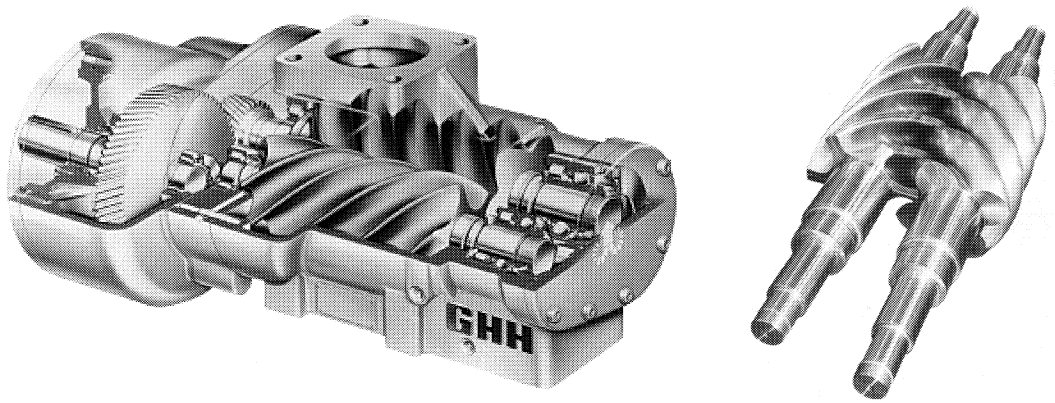

Fig.1: Example of a dry screw compressor design (left) and screw-type machine rotors (right)

This article brings several informations about another kind of undesirable clearance gap in screw-type machines, which is caused by the incorrect contact of rotor teeth screw surfaces, Fig. 1 (right), and new original numerical results of a turbulent leakage flow computation through the two-dimensional computational model of this undesirable clearance gap created by the authors.

The incorrect contact of rotor teeth screw surfaces is induced by the high temperatures and pressures of the fluid compressed in work space chambers. In this study, the incorrect contact is created for the simplicity by a parallel displacement of the male rotor axis that simulates a defect of the correct contact of rotor teeth screw surfaces. The inner deformation of screw surfaces is not involved into the solution and likewise a general position of rotor axes that arises by a real deformation of the machine housing is not accepted. This simplification was necessary for the first step of the numerical solution of this complex problem. The kinematical and geometrical solution of the incorrect contact of rotor teeth screw surfaces was considered as a 3D problem for instantaneous time. The used methodology of the numerical solution presented in this study is valid and available for screw compressors as well as for expanders.

In [13], the laminar computation of the leakage flow through the two-dimensional model of the undesirable clearance gap caused by the incorrect contact of rotor teeth screw surfaces for the prescribed pressure ratio $p_{\text{inlet}}/p_{\text{outlet}} = 2$ was presented. It was assumed that the leakage flow, which is characterized by the reference Reynolds number $Re_\infty = 3900$, through this gap of $100\,\mu$m wide that represents a very narrow channel, could be laminar. But from the obtained numerical results it seems that the assumption of the laminar computation of the gas leakage through the two-dimensional model of this gap is not exactly correct. Therefore the aim of this article is to include the effects of turbulence in a flow field and to perform the turbulent computation of the gas leakage through the two-dimensional model of this undesirable gap.

2. Incorrect contact of screw surfaces

The incorrect contact of screw surfaces σ_2 and σ_3 of the female and male rotors is created by a parallel displacement $\Delta\mathbf{r}_{o_3} = (\Delta x_{o_3}, \Delta y_{o_3}, 0)^{\mathrm{T}}$ of the male rotor axis o_3. The surface σ_3 is displaced in a new position σ_3^Δ, Fig. 2. The first contact of surfaces σ_2 and σ_3^Δ takes place, see Fig. 2, under the conditions

$$ {}_R\mathbf{r}_K \equiv {}_R\mathbf{r}_X \equiv {}^{\sigma_2}_{R}\mathbf{r}_L \quad \wedge \quad {}^{\sigma_2}_{R}\mathbf{n}_L \times {}^{\sigma_3^\Delta}_{R}\mathbf{n}_L = \mathbf{0} \quad \wedge \quad \varphi_3^P = \min\{\varphi_3^P\} \tag{1} $$

at the cross section τ that is defined with $\varphi_3^P = \min\{{}^j\varphi_3^P\}, j \in (1, m)$, where φ_3^P is the angle of rotation of the profile p_3^Δ of the surface σ_3^Δ towards the contact position with the profile p_2 of the surface σ_2 and ${}^{\sigma_2}_{R}\mathbf{n}_L$, ${}^{\sigma_3^\Delta}_{R}\mathbf{n}_L$ are unit normal vectors to the surfaces σ_2 and σ_3^Δ. The curve contact of screw surfaces by their correct meshing changes into a point contact by their incorrect touch.

The generating surface $\sigma_3 = \sigma_3(p_{3L}, \chi)$ is defined by a parametric equation ${}^{\sigma_3}_{R_3}\mathbf{r}_L = {}^{\sigma_3}_{R_3}\mathbf{r}_L(p_{3L}, \chi)$ whose concrete form in the coordinate system $R_3(O_3, \vec{i}_3, \vec{j}_3, \vec{k}_3)$, Fig. 2, is followed

$$ {}^{\sigma_3}_{R_3}\mathbf{r}_L = \mathbf{T}_{R'_3R_3}(-p_{3L}) \cdot \mathbf{T}_{R_{3\gamma}R'_3}(\psi_{3L}) \cdot \begin{bmatrix} r_{\mathrm{S}}\,\sin\varphi - r_{\mathrm{k}}\,\sin\chi \\ -r_{\mathrm{S}}\,\cos\varphi + r_{\mathrm{k}}\,\cos\chi \\ 0 \\ 1 \end{bmatrix} , \tag{2} $$

where $\mathbf{T}_{R_iR_j}$ denotes a transformation matrix from the system R_i to the system R_j.

The conjugate surface $\sigma_2 = \sigma_2(p_{3L}, \chi, \varphi_2)$ is created in the direct envelope way according to the Distelli theorem in the basic coordinate system $R(O, \vec{i}, \vec{j}, \vec{k})$ as

$$ {}^{\sigma_3}_{R}\mathbf{r}_L = \mathbf{T}_{R_\pi R}(\pi) \cdot \mathbf{T}_{R_{30}R_\pi}(-a_w) \cdot \mathbf{T}_{R_3R_{30}}(\varphi_3) \cdot {}^{\sigma_3}_{R_3}\mathbf{r}_L \ . \tag{3} $$

Then the conjugate screw surface σ_2 is described by equations

$$ {}^{\sigma_2}_{R}\mathbf{r}_L = \mathbf{T}_{R_2R}(\varphi_{2k0}) \cdot \mathbf{T}_{RR_2}(\varphi_2) \cdot {}^{\sigma_3}_{R}\mathbf{r}_L \ , \tag{4} $$

$$ {}^{\sigma_3}_{R}\mathbf{n}_L \cdot {}_R\mathbf{v}_{L32} = 0 \ . \tag{5} $$

The equation (5) forms the necessary condition for the contact of both surfaces, i.e. the condition of the perpendicularity of the relative velocity vector ${}_R\mathbf{v}_{L32}$ between the both surfaces and the unit normal vector ${}^{\sigma_3}_{R}\mathbf{n}_L$ in the contact point L. In these equations $\varphi_3 = i_{32}\,\varphi_2$, where i_{32} is the requested transmission ratio. The instantaneous position of rotors, in which

the contact of both surfaces is determined, is defined with angle $\varphi_{3k0} = i_{32}\,\varphi_{2k0}$. The unit normal vector to the screw surface σ_3 in the basic coordinate system $R(O, \vec{i}, \vec{j}, \vec{k})$ is described by the following equations

$$ {}^{\sigma_3}_{R}\mathbf{n}_L = \mathbf{S}_{R_{3\gamma}R} \cdot {}^{\sigma_3}_{R_{3\gamma}}\mathbf{n}_L \ , \tag{6} $$

$$ {}^{\sigma_3}_{R_{3\gamma}}\mathbf{n}_L = \frac{{}_{R_{3\gamma}}\mathbf{t}_1 \times {}_{R_{3\gamma}}\mathbf{t}_2}{|{}_{R_{3\gamma}}\mathbf{t}_1 \times {}_{R_{3\gamma}}\mathbf{t}_2|} \ , \tag{7} $$

where $\mathbf{S}_{R_{3\gamma}R}$ is the matrix expressing the rotational displacement of the system $R_{3\gamma}(O_{3\gamma}, \vec{i}_{3\gamma}, \vec{j}_{3\gamma}, \vec{k}_{3\gamma})$ with respect to the system $R(O, \vec{i}, \vec{j}, \vec{k})$, see Fig. 2, ${}^{\sigma_3}_{R_{3\gamma}}\mathbf{n}_L$ is the unit normal vector to the surface σ_3 in the contact point L expressed in the system $R_{3\gamma}$ and ${}_{R_{3\gamma}}\mathbf{t}_1$, ${}_{R_{3\gamma}}\mathbf{t}_2$ are tangential vectors of the surface σ_3. The relative velocity vector between the both surfaces σ_3 and σ_2 in the contact point L is given by the equation

$$ {}_R\mathbf{v}_{L32} = {}_R\mathbf{v}_{L31} - {}_R\mathbf{v}_{L21} = \mathbf{S}_{R_{3\gamma}R} \cdot {}_{R_{3\gamma}}\mathbf{v}_{L31} - {}_R\boldsymbol{\omega}_{21} \times {}_R\mathbf{r}_L $$

expressed in the basic coordinate system $R(O, \vec{i}, \vec{j}, \vec{k})$.

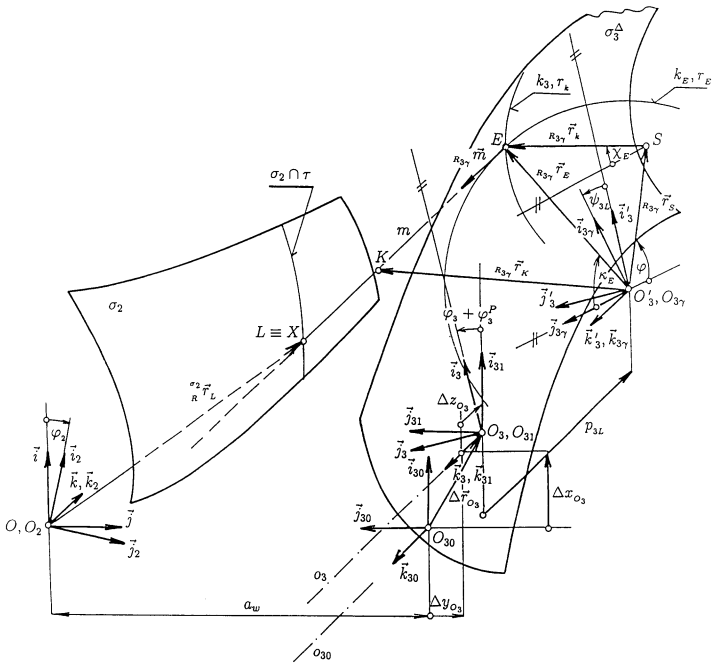

Fig.2: Searching of the incorrect contact of screw surfaces σ_2 a σ_3^{Δ}

For the numerical solution of the incorrect contact of screw surfaces σ_2 and σ_3^{Δ}, the following basic geometrical parameters of a screw-type machine were considered: the axis distance $a_w = 100\,\text{mm}$, the gear ratio $i_{32} = 1.5$, the helix angle on the rolling cylinder of both rotors $\gamma = 45°$, the radius $r_\text{k} = 125$ mm of the circle $k_3(S, r_\text{k})$, Fig. 2, which represents the profile p_3^{Δ} of the surface σ_3^{Δ}, displacements $\Delta x_{o_3} = 0.1\,\text{mm}$ and $\Delta y_{o_3} = 0.1\,\text{mm}$ of the male rotor axis o_3. The incorrect contact of screw surfaces σ_2 and σ_3^{Δ} of both rotor teeth is visualized in Fig. 3, where CH_{32} is the contact point and m_2, m_3 are curves of the minimum

distance of the surfaces σ_2 and σ_3^{Δ}. In consequence of the parallel displacement of the male rotor axis o_3, the curve contact, in which the both screw surfaces touch each other correctly, changes into the contact at the isolated point CH_{32}, Fig. 3. The contact of screw surfaces σ_2 and σ_3^{Δ} in the point CH_{32} is at the cross section for $z = 34.04\,\text{mm}$.

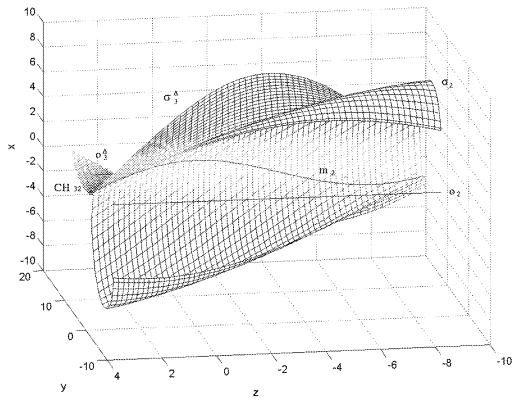

Fig.3: Numerical simulation of the incorrect contact of rotor teeth screw surfaces σ_2 and σ_3^{Δ}

The situation at the cross section for $z = -68\,\text{mm}$ is displayed in Fig. 4 (left). The detail of the undesirable gap caused by the incorrect contact of screw surfaces σ_2 and σ_3^{Δ} is shown in Fig. 4 (right).

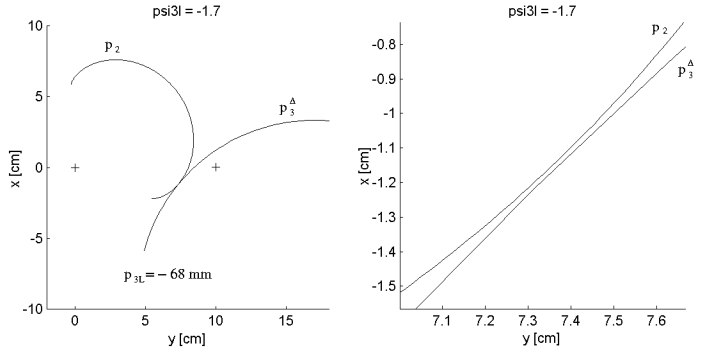

Fig.4: The cross section of screw surfaces σ_2 and σ_3^{Δ} for $z = -68\,mm$ (left) and the detail of the undesirable gap caused by the incorrect contact (right)

The computational model of the gap caused by the incorrect contact of rotor teeth screw surfaces σ_2 and σ_3^{Δ} represents a two-dimensional bounded domain $\Omega \subset R^2$ at the cross section for $z = -68\,\text{mm}$ Fig. 4 (right) or Fig. 5 (left). The computational domain boundary is described as $\partial\Omega = \partial\Omega_I \cup \partial\Omega_O \cup \partial\Omega_W$, where $\partial\Omega_I$ is the inlet, $\partial\Omega_O$ is the outlet and $\partial\Omega_W = \partial\Omega_W^{p_2} \cup \partial\Omega_W^{p_3^{\Delta}}$ are impermeable walls of the computational domain $\Omega \subset R^2$ corresponding to the profiles p_2 and p_3^{Δ}. The profiles p_2 and p_3^{Δ} create the upper and lower curves of the two-dimensional computational model of the undesirable gap, Fig. 4.

3. Mathematical model of a turbulent compressible fluid flow

Let $\Omega \subset R^2$ be a computational domain and $(0, \mathcal{T})$ a time interval. The fundamental equations for unsteady laminar flow of a compressible viscous heat-conducting Newtonian fluid in an absolute frame of reference are derived from the integral form of the conservation laws for mass, momentum and total energy in Eulerian description, [2]. The resulting system of the governing equations is known as the non-linear conservative system of the Navier-Stokes equations described in [12]. For most compressible flows of practical importance, the flow is turbulent. In order to obtain the governing conservation equations for turbulent compressible flow, it is convenient to replace the instantaneous quantities in the system of the Navier-Stokes equations by their mean and their fluctuating values.

If $\Phi(\mathbf{y}, t)$ is any time dependent flow variable, two different types of averaging of $\Phi(\mathbf{y}, t)$ can be defined:

– conventional time averaging introduced by Reynolds in which the instantaneous flow variable $\Phi(\mathbf{y}, t)$ is expressed as the sum of a mean $\overline{\Phi}(\mathbf{y}, t)$ and a fluctuating part $\Phi'(\mathbf{y}, t)$, so that

$$\Phi(\mathbf{y},t) = \overline{\Phi}(\mathbf{y}, t) + \Phi'(\mathbf{y}, t) \ , \tag{9}$$

$$\overline{\Phi}(\mathbf{y},t) = \frac{1}{\Delta t} \int\limits_{t_0}^{t_0+\Delta t} \Phi(\mathbf{y}, t)\, \mathrm{d}t \ . \tag{10}$$

– mass-weighted time averaging suggested by Favre in which the instantaneous flow variable $\Phi(\mathbf{y}, t)$ is decomposed into the mass-averaged part $\widetilde{\Phi}(\mathbf{y}, t)$ and a fluctuating part $\Phi''(\mathbf{y}, t)$, wherefore

$$\Phi(\mathbf{y}, t) = \widetilde{\Phi}(\mathbf{y}, t) + \Phi''(\mathbf{y}, t) \ , \tag{11}$$

$$\widetilde{\Phi}(\mathbf{y}, t) = \frac{\overline{\varrho\, \Phi}}{\overline{\varrho}} \ , \tag{12}$$

where the bar denotes conventional time averaging. Note the important differences between the two averaging procedures. In the conventional time averaging, $\overline{\Phi'} = 0$ and $\overline{\varrho\, \Phi'} \neq 0$; in the mass-weighted averaging, $\overline{\Phi''} \neq 0$ and $\overline{\varrho\, \Phi''} = 0$.

Introducing a conventional time average decomposition (9) of density ϱ and static pressure p and a mass-weighted time average decomposition (11) of the velocity vector $\mathbf{v} = (v_1, v_2)^{\mathrm{T}}$, total energy E per unit volume and thermodynamic temperature T and application of the averaging operations described precisely in [11], produce the non-linear system of the Favre-averaged Navier-Stokes equations (FANS) written in non-dimensional conservative form as

$$\frac{\partial \mathbf{w}}{\partial t} + \sum_{j=1}^{2} \frac{\partial \boldsymbol{\mathcal{F}}_j^{\mathrm{I}}(\mathbf{w})}{\partial y_j} = \frac{1}{Re_\infty} \sum_{j=1}^{2} \frac{\partial \boldsymbol{\mathcal{F}}_j^{\mathrm{V}}(\mathbf{w})}{\partial y_j} \quad \text{in} \quad \Omega \times (0, \mathcal{T}) \ , \tag{13}$$

where t is time, $\mathbf{y} = (y_1, y_2)^{\mathrm{T}}$ is the vector of Cartesian space coordinates and $Re_\infty = \varrho_{\mathrm{ref}}\, u_{\mathrm{ref}}\, l_{\mathrm{ref}}/\eta_{\mathrm{ref}}$ is the reference Reynolds number. The column vector $\mathbf{w}$ of conservative variables and the vectors $\boldsymbol{\mathcal{F}}_j^{\mathrm{I}}(\mathbf{w})$ of inviscid and $\boldsymbol{\mathcal{F}}_j^{\mathrm{V}}(\mathbf{w})$ of viscous fluxes are given by

$$\mathbf{w}(\mathbf{y}, t) = (w_1, w_2, w_3, w_4)^{\mathrm{T}} = (\overline{\varrho}, \overline{\varrho}\, \widetilde{v}_1, \overline{\varrho}\, \widetilde{v}_2, \widetilde{E})^{\mathrm{T}} \ , \qquad \mathbf{y} \in \Omega \ , \quad t \in (0, \mathcal{T}) \ , \tag{14}$$

$$\boldsymbol{\mathcal{F}}_j^{\mathrm{I}}(\mathbf{w}) = (\overline{\varrho}\, \widetilde{v}_j, \overline{\varrho}\, \widetilde{v}_1\, \widetilde{v}_j + \overline{p}\, \delta_{1j}, \overline{\varrho}\, \widetilde{v}_2\, \widetilde{v}_j + \overline{p}\, \delta_{2j}, (\widetilde{E} + \overline{p})\, \widetilde{v}_j)^{\mathrm{T}} \ , \qquad j = 1, 2 \ , \tag{15}$$

$$\boldsymbol{\mathcal{F}}_j^{\mathrm{V}}(\mathbf{w}) = (0, \widetilde{\tau}_{1j}, \widetilde{\tau}_{2j}, \widetilde{\tau}_{1j}\, \widetilde{v}_1 + \widetilde{\tau}_{2j}\, \widetilde{v}_2 - \widetilde{q}_j)^{\mathrm{T}} \ , \qquad j = 1, 2 \ , \tag{16}$$

where δ_{ij} is Kronecker delta. The shear stresses $\widetilde{\tau}_{ij}$ and the heat flux vectors $\widetilde{q}_j$ in (16) can be expressed as

$$\widetilde{\tau}_{ij} = \widetilde{\tau}_{ij}^{\mathrm{lam}} - \overline{\varrho\, v_i'' \, v_j''} \equiv (\eta + \eta_{\mathrm{t}}) \left(\frac{\partial \widetilde{v}_i}{\partial y_j} + \frac{\partial \widetilde{v}_j}{\partial y_i} - \frac{2}{3}\, \delta_{ij}\, \frac{\partial \widetilde{v}_k}{\partial y_k} \right) , \qquad j = 1, 2 , \tag{17}$$

$$\widetilde{q}_j = \widetilde{q}_j^{\mathrm{lam}} + c_{\mathrm{p}}\, \overline{\varrho\, T\, v_j''} \equiv -\frac{\kappa}{\kappa - 1} \left(\frac{\eta}{Pr} + \frac{\eta_{\mathrm{t}}}{Pr_{\mathrm{t}}} \right) \frac{\partial}{\partial y_j} \left(\frac{\overline{p}}{\overline{\varrho}} \right) , \qquad j = 1, 2 . \tag{18}$$

Since the fluctuating component of the molecular viscosity η is usually small, it has been neglected. In order to close the non-linear system (13) of the governing equations, the turbulent shear stresses $\widetilde{\tau}_{ij}^{\mathrm{turb}} \equiv -\overline{\varrho\, v_i'' \, v_j''}$ in (17) are modelled using the Boussinesq eddy-viscosity approximation [4], where the concept of a turbulent (or eddy) viscosity η_{t} is introduced. The turbulent heat flux vectors $\widetilde{q}_j^{\mathrm{turb}} \equiv c_{\mathrm{p}}\, \overline{\varrho\, T\, v_j''}$ in (18) are modelled using a gradient approximation written in a form such as to resemble the laminar heat flux vectors. For this purpose, a turbulent Prandtl number Pr_{t} is defined. The turbulent Prandtl number is usually assumed constant and for wall bounded flows is $Pr_{\mathrm{t}} = 0.9$.

Assuming a calorically perfect gas, the static pressure is given by the equation of state

$$\overline{p} = \overline{\varrho}\, r\, \widetilde{T} = (\kappa - 1)\, \overline{\varrho}\, c_{\mathrm{v}}\, \widetilde{T} \equiv (\kappa - 1) \left(\widetilde{E} - \frac{1}{2}\, \overline{\varrho}\, \widetilde{v}_j\, \widetilde{v}_j \right) , \tag{19}$$

where $r = c_{\mathrm{p}} - c_{\mathrm{v}}$ is the gas constant per unit mass, c_{p} and c_{v} are the specific heats at constant pressure and volume, respectively and $\kappa = 1.4$ is Poisson's constant. The laminar Prandtl number defined as $Pr = c_{\mathrm{p}}\, \eta / k = 0.72$ is taken to be a constant for a calorically perfect gas, where η is molecular viscosity and k is thermal conductivity. The external volume forces are not considered in our case. It rests to determine the turbulent viscosity η_{t}.

The complexity of our problem motivates the use of relatively simple turbulence models. The advantage of algebraic models is that no additional transport differential equations have to be solved. The description of algebraic turbulence models can be found in e.g. [16] or [4]. For the computation of the turbulent viscosity η_{t}, the algebraic turbulence model introduced by Baldwin and Lomax [5] is considered. It is a two-layer turbulence model, based on the mixing-length hypothesis, which is formulated for use in computations where boundary-layer properties such as the boundary-layer thickness δ, the kinetic displacement thickness δ_v^* and the boundary-layer edge velocity u_{e} are difficult to determine. This situation often arises in numerical simulation of separated flows. The turbulent viscosity η_{t} is given by using a two-layer approach,

$$\eta_{\mathrm{t}} = \begin{cases} \eta_{\mathrm{t_i}} & \text{if} \quad y \le y_{\mathrm{m}} \quad \ldots \text{ inner layer} \\ \eta_{\mathrm{t_o}} & \text{if} \quad y > y_{\mathrm{m}} \quad \ldots \text{ outer layer} \end{cases} , \tag{20}$$

where y is the normal distance from the wall and y_{m} is the smallest value of y for which $\eta_{\mathrm{t_i}} = \eta_{\mathrm{t_o}}$. For the wake region, the inner layer is not defined so we have $\eta_{\mathrm{t}} = \eta_{\mathrm{t_o}}$. In the inner layer, $\eta_{\mathrm{t_i}}$ is computed as follows

$$\eta_{\mathrm{t_i}} = \overline{\varrho}\, l_{\mathrm{mix}}^2\, |\omega| , \tag{21}$$

$$l_{\mathrm{mix}} = \gamma\, y\, F_{\mathrm{D}} , \qquad F_{\mathrm{D}} = 1 - \mathrm{e}^{-y^+ / A^+} , \qquad \omega = \frac{\partial \widetilde{u}}{\partial y} - \frac{\partial \widetilde{v}}{\partial x} , \tag{22}$$

where γ is the von Karman constant, the mixing length l_{mix} is determined by the van Driest function F_{D} and ω is the vorticity. The non-dimensional space coordinate y^+, normal to the wall, can be written as

$$y^+ = \frac{y}{\eta_{\mathrm{w}}} \sqrt{\overline{\varrho}_{\mathrm{w}} \, |\widetilde{\tau}_{\mathrm{w}}|} \; , \qquad \widetilde{\tau}_{\mathrm{w}} = \eta_{\mathrm{w}} \left. \frac{\partial \widetilde{u}}{\partial y} \right|_{y=0} \; , \tag{23}$$

where $\widetilde{\tau}_{\mathrm{w}}$ is the wall shear stress in the direction of the flow and the subscript w indicates the wall quantities. In the outer layer, $\eta_{\mathrm{t_o}}$ is given by

$$\eta_{\mathrm{t_o}} = \overline{\varrho} \, \alpha \, C_{\mathrm{cp}} \, F_{\mathrm{wake}} \, F_{\mathrm{kleb}} \; , \tag{24}$$

$$F_{\mathrm{wake}} = \min \left(y_{\max} \, G_{\max}, C_{\mathrm{wake}} \, y_{\max} \, \frac{(\Delta V)^2}{G_{\max}} \right) \; , \qquad G_{\max} = \max_{y} (y \, |\omega| \, F_{\mathrm{D}}) \; , \tag{25}$$

where $y_{\max}$ is the value of y where $G_{\max}$ occurs, $G(y_{\max}) = G_{\max}$, and ΔV is the difference between the absolute values of the maximum and minimum velocities in the profile. For wall bounded flows, the minimum velocity occurs at the wall where the velocity is zero, then $\Delta V = (\widetilde{u}^{\,2} + \widetilde{v}^{\,2})^{1/2}_{\max}$. For shear layer flows, ΔV is defined as the difference between the maximum velocity in the layer and the velocity at the $y_{\max}$ location, that is, $\Delta V = (\widetilde{u}^{\,2} + \widetilde{v}^{\,2})^{1/2}_{\max} - (\widetilde{u}^{\,2} + \widetilde{v}^{\,2})^{1/2}_{y_{\max}}$ for the direction normal to the wall. The Klebanoff's intermittency factor F_{kleb} is given by

$$F_{\mathrm{kleb}} = \left[1 + 5.5 \left(C_{\mathrm{kleb}} \, \frac{y}{y_{\max}} \right)^6 \right]^{-1} \; . \tag{26}$$

The typical model constants $\gamma = 0.4$, $A^+ = 26$, $\alpha = 0.0168$, $C_{\mathrm{cp}} = 1.6$, $C_{\mathrm{wake}} = 0.25$ and $C_{\mathrm{kleb}} = 0.3$, [16] or [4], are used in our case. Finally, the turbulent viscosity distribution across the boundary layer is determined as

$$\eta_{\mathrm{t}} = \min(\eta_{\mathrm{t_i}}, \eta_{\mathrm{t_o}}) \; . \tag{27}$$

To simulate transition from laminar to turbulent flow, Baldwin and Lomax proposed [5] to set η_{t} equal to zero everywhere in a wall-normal profile for which the maximum tentatively computed value of η_{t} from the foregoing relations is less than a pre-specified value, that is,

$$\eta_{\mathrm{t}} = 0 \quad \text{if} \quad (\eta_{\mathrm{t}})_{\max \text{ in a profile}} < C_{\mathrm{MUTM}} \cdot \eta_{\mathrm{ref}} \tag{28}$$

with a proposed value of $C_{\mathrm{MUTM}} = 14$. To initiate a turbulent computation, the initial value of the turbulent viscosity is set equal to zero everywhere within the computational domain. Subsequently the turbulent viscosity is computed from (27) and (28) and is updated after each time step. For the wake region, the inner layer is not defined, so $\eta_{\mathrm{t_i}} := \infty$.

4. Numerical method

To solve the non-linear conservative system of the Favre-averaged Navier-Stokes equations (13), the same numerical method as for the system of the compressible Navier-Stokes equations is used, [12], only the viscous coefficient is replaced by the sum of the molecular and turbulent viscosities. The turbulent viscosity η_{t} is computed using the algebraic

Baldwin-Lomax turbulence model which is mathematically simple and its implementation into the own developed numerical code for the laminar flow computation is easy.

For the discretization of the system of the Favre-averaged Navier-Stokes equations (13), the cell-centred finite volume method on a structured quadrilateral grid, [2] and [12], is used. Time integration of the inviscid part of the system (13) is realized by the finite volume formulation of the most widely used explicit two-step TVD MacCormack scheme. The approximation $\mathrm{Visc}(\mathbf{w}_{ij})$ of the viscous part of the system (13) is modelled using a finite volume version of central differences on dual cells, see [12] for details, and is added to the predictor and corrector steps of the MacCormack scheme

$$\mathbf{w}_{ij}^{n+\frac{1}{2}} = \mathbf{w}_{ij}^{n} - \frac{\Delta t}{|\Omega_{ij}|} \sum_{m=1}^{4} \left(\mathbf{f}_m^n \, S_m^{\mathrm{x}} + \mathbf{g}_m^n \, S_m^{\mathrm{y}} \right) + \frac{\Delta t}{|\Omega_{ij}|} \, \mathrm{Visc}(\mathbf{w}_{ij}^{n}) \; , \tag{29}$$

$$\overline{\mathbf{w}_{ij}^{n+1}} = \frac{1}{2} \left\{ \mathbf{w}_{ij}^{n} + \mathbf{w}_{ij}^{n+\frac{1}{2}} - \frac{\Delta t}{|\Omega_{ij}|} \sum_{m=1}^{4} \left(\mathbf{f}_m^{n+\frac{1}{2}} S_m^{\mathrm{x}} + \mathbf{g}_m^{n+\frac{1}{2}} S_m^{\mathrm{y}} \right) \right\} + \frac{1}{2} \frac{\Delta t}{|\Omega_{ij}|} \, \mathrm{Visc}(\mathbf{w}_{ij}^{n+\frac{1}{2}}) \; , \tag{30}$$

$$\mathbf{w}_{ij}^{n+1} = \overline{\mathbf{w}_{ij}^{n+1}} + {}^{(\mathrm{TVD})}\mathbf{w}_{ij}^{1n} + {}^{(\mathrm{TVD})}\mathbf{w}_{ij}^{2n} \; , \tag{31}$$

where $\mathbf{w}_{ij}^{n+1}$ is the corrected numerical solution at time t_{n+1} and $|\Omega_{ij}|$ denotes the face area of the finite volume Ω_{ij}. The vectors $\mathbf{f}_m \equiv \boldsymbol{\mathcal{F}}_{1m}^{\mathrm{I}}$ and $\mathbf{g}_m \equiv \boldsymbol{\mathcal{F}}_{2m}^{\mathrm{I}}$ of the inviscid numerical fluxes through the edges Γ_{ij}^m, $m = 1, \ldots, 4$, of the cell Ω_{ij} at time t_n are evaluated as

$$\begin{aligned} &\mathbf{f}_1^n = \mathbf{f}(\mathbf{w}_{i+1j}^n) \; , \qquad \mathbf{f}_2^n = \mathbf{f}(\mathbf{w}_{ij+1}^n) \; , \qquad \mathbf{f}_3^n \equiv \mathbf{f}_4^n = \mathbf{f}(\mathbf{w}_{ij}^n) \; , \\ &\mathbf{g}_1^n = \mathbf{g}(\mathbf{w}_{i+1j}^n) \; , \qquad \mathbf{g}_2^n = \mathbf{g}(\mathbf{w}_{ij+1}^n) \; , \qquad \mathbf{g}_3^n \equiv \mathbf{g}_4^n = \mathbf{g}(\mathbf{w}_{ij}^n) \end{aligned}$$

and at time $t_{n+\frac{1}{2}}$ as

$$\begin{aligned} &\mathbf{f}_1^{n+\frac{1}{2}} \equiv \mathbf{f}_2^{n+\frac{1}{2}} = \mathbf{f}(\mathbf{w}_{ij}^{n+\frac{1}{2}}) \; , \qquad \mathbf{f}_3^{n+\frac{1}{2}} = \mathbf{f}(\mathbf{w}_{i-1j}^{n+\frac{1}{2}}) \; , \qquad \mathbf{f}_4^{n+\frac{1}{2}} = \mathbf{f}(\mathbf{w}_{ij-1}^{n+\frac{1}{2}}) \; , \\ &\mathbf{g}_1^{n+\frac{1}{2}} \equiv \mathbf{g}_2^{n+\frac{1}{2}} = \mathbf{g}(\mathbf{w}_{ij}^{n+\frac{1}{2}}) \; , \qquad \mathbf{g}_3^{n+\frac{1}{2}} = \mathbf{g}(\mathbf{w}_{i-1j}^{n+\frac{1}{2}}) \; , \qquad \mathbf{g}_4^{n+\frac{1}{2}} = \mathbf{g}(\mathbf{w}_{ij-1}^{n+\frac{1}{2}}) \; . \end{aligned}$$

$\mathbf{S}_m = (S_m^{\mathrm{x}}, S_m^{\mathrm{y}})^{\mathrm{T}}$ are cell side normal vectors to the edges Γ_{ij}^m, where we designate $\mathbf{S}_1 = \mathbf{S}_{i+\frac{1}{2}j}$, $\mathbf{S}_2 = \mathbf{S}_{ij+\frac{1}{2}}$, $\mathbf{S}_3 = \mathbf{S}_{i-\frac{1}{2}j}$ and $\mathbf{S}_4 = \mathbf{S}_{ij-\frac{1}{2}}$. The added one-dimensional TVD-type viscosity term ${}^{(\mathrm{TVD})}\mathbf{w}_{ij}^{1n}$ in the direction of the change of index i in (31), proposed by Causon [6], is given by

$${}^{(\mathrm{TVD})}\mathbf{w}_{ij}^{1n} = [P_{ij}^{+} + P_{i+1j}^{-}] \, (\mathbf{w}_{i+1j}^{n} - \mathbf{w}_{ij}^{n}) - [P_{i-1j}^{+} + P_{ij}^{-}] \, (\mathbf{w}_{ij}^{n} - \mathbf{w}_{i-1j}^{n}) \; , \tag{32}$$

$$P_{ij}^{\pm} \equiv P(r_{ij}^{\pm}) = \frac{1}{2} \, C(\nu_{ij}) \, [1 - \Phi(r_{ij}^{\pm})] \; , \tag{33}$$

$$r_{ij}^{+} = \frac{(\mathbf{w}_{i+1j}^{n} - \mathbf{w}_{ij}^{n}, \mathbf{w}_{ij}^{n} - \mathbf{w}_{i-1j}^{n})}{(\mathbf{w}_{i+1j}^{n} - \mathbf{w}_{ij}^{n}, \mathbf{w}_{i+1j}^{n} - \mathbf{w}_{ij}^{n})} \; , \qquad r_{ij}^{-} = \frac{(\mathbf{w}_{i+1j}^{n} - \mathbf{w}_{ij}^{n}, \mathbf{w}_{ij}^{n} - \mathbf{w}_{i-1j}^{n})}{(\mathbf{w}_{ij}^{n} - \mathbf{w}_{i-1j}^{n}, \mathbf{w}_{ij}^{n} - \mathbf{w}_{i-1j}^{n})} \; .$$

Note that in these relations $(\cdot, \cdot)$ denotes the scalar product of two vectors. The flux limiter $\Phi(r_{ij}^{\pm})$ and the function $C(\nu_{ij})$ in relation (33) are defined as

$$\Phi(r_{ij}^{\pm}) = \begin{cases} \min(2r_{ij}^{\pm}, 1) & \text{for} \quad r_{ij}^{\pm} > 0 \\ 0 & \text{for} \quad r_{ij}^{\pm} \le 0 \end{cases} \; , \qquad C(\nu_{ij}) = \begin{cases} \nu_{ij}(1 - \nu_{ij}) & \text{for} \quad \nu_{ij} \le \frac{1}{2} \\ 0.25 & \text{for} \quad \nu_{ij} > \frac{1}{2} \end{cases} \tag{34}$$

and ν_{ij} is given by the formula

$$\nu_{ij} = \frac{\Delta t}{\Delta x_{ij}} \left(|\widetilde{u}_{ij}| + \widetilde{a}_{ij} \right) , \tag{35}$$

where $\widetilde{u}_{ij}$ is the velocity and $\widetilde{a}_{ij}$ is the local speed of sound. The time step Δt is given by the following CFL condition (36) and Δx_{ij}, Δy_{ij} are the approximations of the lengths of the cell Ω_{ij}. For the added dissipative term ${}^{(\mathrm{TVD})}\mathbf{w}_{ij}^{2n}$ in the equation (31), similar formulae with the shifting of index j are used.

A necessary CFL stability condition of the explicit two-step MacCormack scheme in non-dimensional form is expressed by the restriction for the time step

$$\Delta t \leq \min_{i,j} \mathrm{CFL} \left[\frac{|\widetilde{u}_{ij}| + \widetilde{a}_{ij}}{\Delta x_{ij}} + \frac{|\widetilde{v}_{ij}| + \widetilde{a}_{ij}}{\Delta y_{ij}} + \frac{2}{Re_\infty} \left(\frac{1}{\Delta x_{ij}^2} + \frac{1}{\Delta y_{ij}^2} \right) \right]^{-1} , \tag{36}$$

where $|\widetilde{u}_{ij}| + \widetilde{a}_{ij}$ and $|\widetilde{v}_{ij}| + \widetilde{a}_{ij}$ are maximum absolute values of the eigenvalues of Jacobian matrices $\mathbf{A}(\mathbf{w}_{ij}) = \partial \mathbf{f}(\mathbf{w}_{ij})/\partial \mathbf{w}_{ij}$ and $\mathbf{B}(\mathbf{w}_{ij}) = \partial \mathbf{g}(\mathbf{w}_{ij})/\partial \mathbf{w}_{ij}$ and the constant $\mathrm{CFL} \in (0, 1)$.

5. Numerical results

For the turbulent leakage flow computation in the considered two-dimensional model of the undesirable clearance gap caused by the incorrect contact of rotor teeth screw surfaces, Fig. 5 (left), the relatively fine structured quadrilateral grid with 190×64 cells was used. The detail of the computational grid is shown in Fig. 5 (right). In order to resolve the boundary layer with sufficient accuracy, the computational grid was refined in the direction normal to the walls. The width of the first cell at the wall is

$$\Delta y_1 = \frac{0.05}{\sqrt{Re_\infty}} \tag{37}$$

and the other cells in the vicinity of the solid wall have the width given by the formula

$$\Delta y_{s+1} = (1 + \mathrm{A})\, \Delta y_s \ . \tag{38}$$

For this case we set $\mathrm{A} = 0.17$ and $s = 1, \ldots, 28$.

The problem was solved for the reference Reynolds number $Re_\infty = 3900$ as a non-stationary turbulent compressible Newtonian fluid flow considering the following non-dimensional boundary conditions. At the inlet $\partial\Omega_I$, the total pressure $\overline{p}_{01} = 1$, the total temperature $\widetilde{T}_{01} = 1$, the inlet angle α_1, $\partial \widetilde{T}/\partial \mathbf{n} = 0$ and $\sum_{j=1}^{2} \widetilde{\tau}_{ij}\, n_j = 0$, $i = 1{,}2$ were prescribed. At the outlet $\partial\Omega_O$, the static pressure $\overline{p}_2 = 0.5$, $\partial \widetilde{T}/\partial \mathbf{n} = 0$ and $\sum_{j=1}^{2} \widetilde{\tau}_{ij}\, n_j = 0$, $i = 1{,}2$ were kept. On the solid walls $\partial\Omega_W^{p_2}$ and $\partial\Omega_W^{p_3^\Delta}$, the boundary conditions $\widetilde{u} = 0$, $\widetilde{v} = 0$ and $\partial \widetilde{T}/\partial \mathbf{n} = 0$ were satisfied. $\mathbf{n}$ is the outward unit normal vector to the boundary. Note that for this turbulent computation the same computational grid, the same reference Reynolds number and the same boundary conditions as for the laminar computation, see [13], were used. The free stream conditions over the entire computational domain $\Omega \subset R^2$ were imposed to initialize the explicit TVD MacCormack scheme (29)–(31). The parameter $\mathrm{CFL} = 0.5$ in the stability condition (36) was chosen.

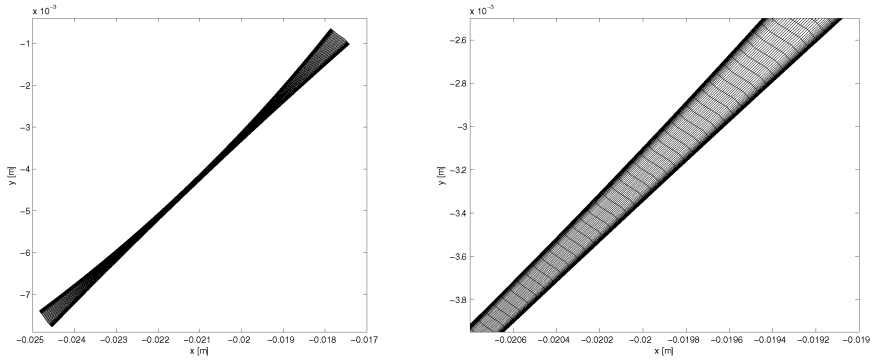

Fig.5: Computational domain $\Omega \subset R^2$ (left) and detail of the structured quadrilateral grid with 190×64 cells (right)

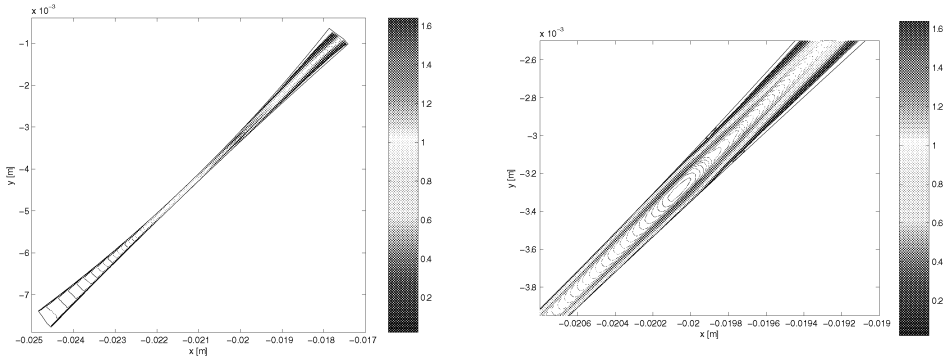

Fig.6: Isolines of the Mach number (left) and their detail (right) for the turbulent flow computation

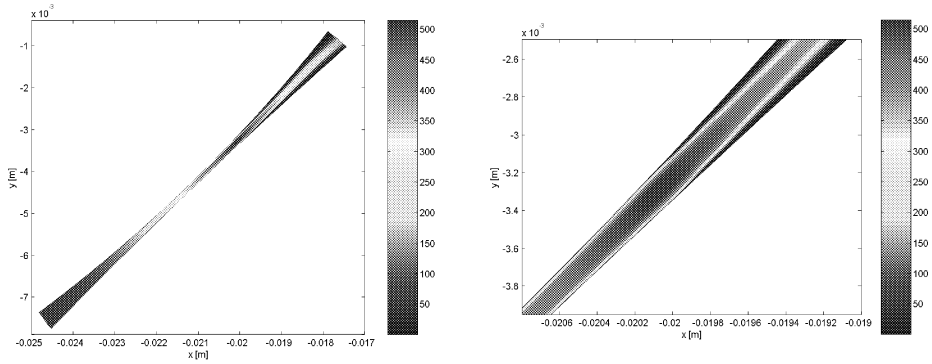

Fig.7: Velocity magnitude distribution in [m/s] (left) and its detail (right) for the turbulent flow computation

Fig. 6 displays the isolines of the Mach number distribution in the gap plotted with step $\Delta M = 0.02$ and computed at time $t = 8.26{\cdot}10^{-5}$ s using the numerical method described in this study. The velocity magnitude distribution at the same time is shown in Fig. 7. It is obvious that the leakage flow in the two-dimensional model of the gap caused by the incorrect contact of rotor teeth screw surfaces is transonic ($M_{\max} \approx 1.6$) for the prescribed pressure ratio $p_{\text{inlet}}/p_{\text{outlet}} = 2$ but without shock waves.

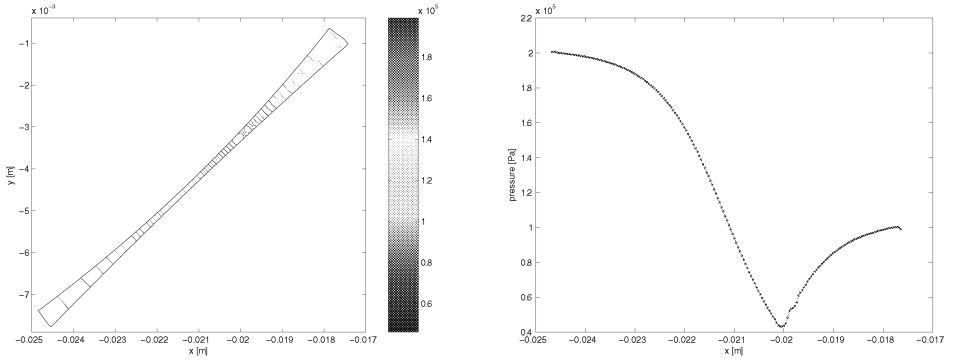

Fig.8: Isolines of the static pressure in [Pa] (left) and the static pressure distribution along a middle streamline (right) for the turbulent flow computation

The isolines of the static pressure plotted with step $\Delta p = 3500\,\mathrm{Pa}$ and the static pressure distribution along a middle streamline of the gap computed at time $t = 8.26{\cdot}10^{-5}\,\mathrm{s}$ using the turbulent flow computation are visualized in Fig. 8. It can be seen that the prescribed pressure ratio $p_{\mathrm{inlet}}/p_{\mathrm{outlet}} = 2$ is satisfied.

For reference only, the isolines of the Mach number distribution in the two-dimensional computational model of the gap plotted with step $\Delta M = 0.02$ at times $t_1 = 2.798{\cdot}10^{-4}\,\mathrm{s}$, $t_2 = 2.845{\cdot}10^{-4}\,\mathrm{s}$ and $t_3 = 2.916{\cdot}10^{-4}\,\mathrm{s}$ obtained using the laminar flow computation presented in [13] are shown in Fig. 9. The non-stationarities (the changes in the shape of the wake) can be observed in the laminar case and the maximum values of the Mach number oscillates within the interval $M_{\max} \in \langle 1.1, 1.48\rangle$. Fig. 10 displays the isolines of the static pressure plotted with step $\Delta p = 3500\,\mathrm{Pa}$ and the static pressure distributions along a middle streamline of the two-dimensional computational model of the gap at times $t_1 = 2.798{\cdot}10^{-4}\,\mathrm{s}$, $t_2 = 2.845{\cdot}10^{-4}\,\mathrm{s}$ and $t_3 = 2.916{\cdot}10^{-4}\,\mathrm{s}$ gained using the laminar flow computation presented in [13].

The value $\dot{m} = 0.0445\,\mathrm{kg\,m^{-1}s^{-1}}$ of the mass flow rate per unit height through the narrowest position of this two-dimensional computational model of the undesirable gap caused by the incorrect contact of rotor teeth screw surfaces was determined for the turbulent flow computation. For completeness' sake, the following graph of the values of the mass flow rate per unit height through this model of the gap in dependence on the time was plotted, Fig. 11, for the laminar flow computation presented in [13].

6. Conclusions

The preliminary analysis of the incorrect contact of screw-type machine rotor teeth surfaces caused by a parallel displacement of the male rotor axis is described in this study. It is shown that the curve contact of screw surfaces by their correct meshing changes into the point contact by their incorrect touch. The simplified two-dimensional computational model of the undesirable gap caused by this incorrect contact of rotor teeth screw surfaces is created by the authors and the numerical method for the statistically steady turbulent computation of the leakage flow through this two-dimensional model of the gap based on the cell-centred finite volume formulation of the explicit two-step MacCormack scheme defined on a structured quadrilateral grid is presented.

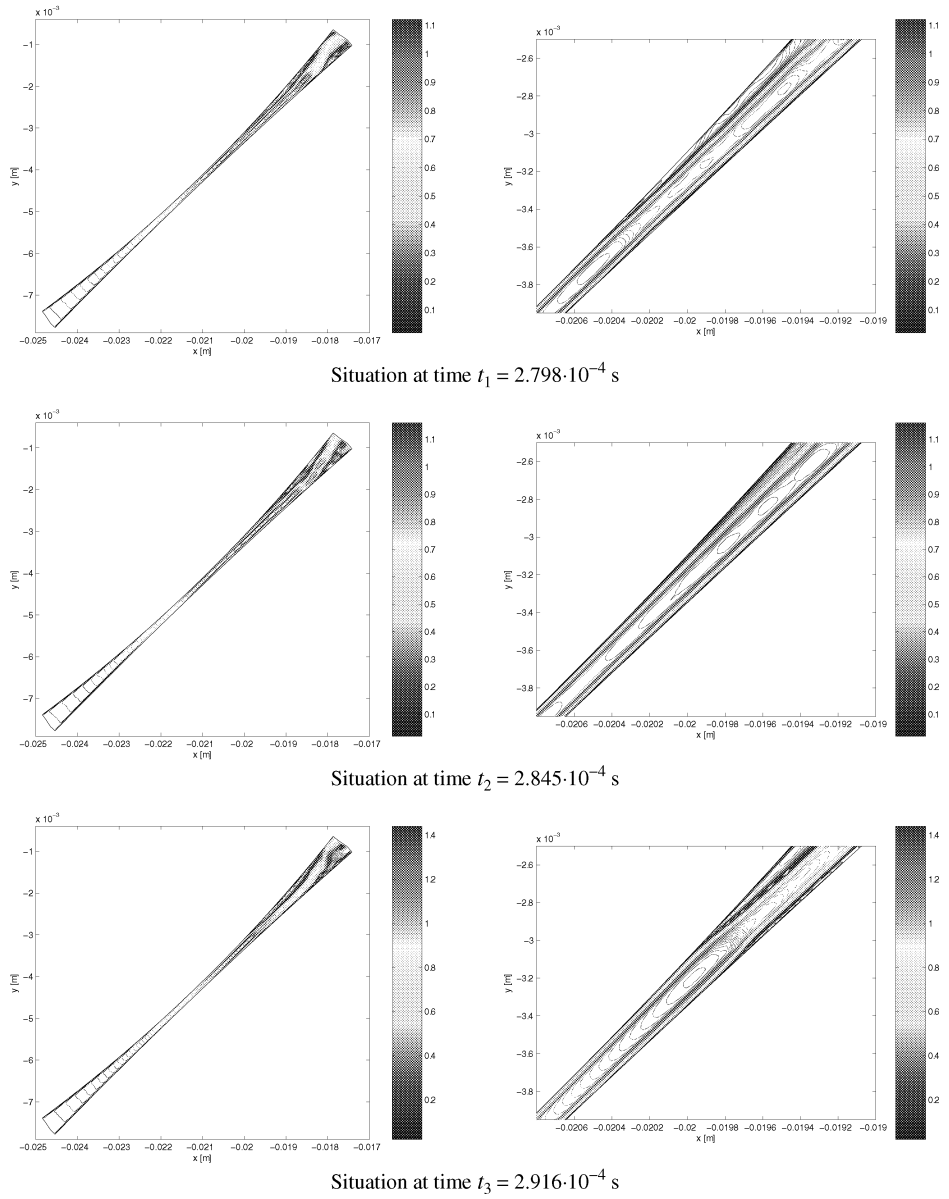

Fig.9: Isolines of the Mach number (left) and their detail (right) for the laminar flow computation

The original results computed using the numerical code developed by the author demonstrate that the leakage flow through the two-dimensional model of the undesirable clearance gap of 100 μm wide caused by the incorrect contact of rotor teeth screw surfaces is transonic ($M_{\max} \approx 1.6$) for the prescribed pressure ratio $p_{\text{inlet}}/p_{\text{outlet}} = 2$ but without shock waves typical for transonic flows [1] at macroscales. That is probably result of the viscous fluid flow in the very narrow channel, where the viscous forces prevail over the inertial forces. The value of the mass flow rate per unit height through this two-dimensional model of the gap is

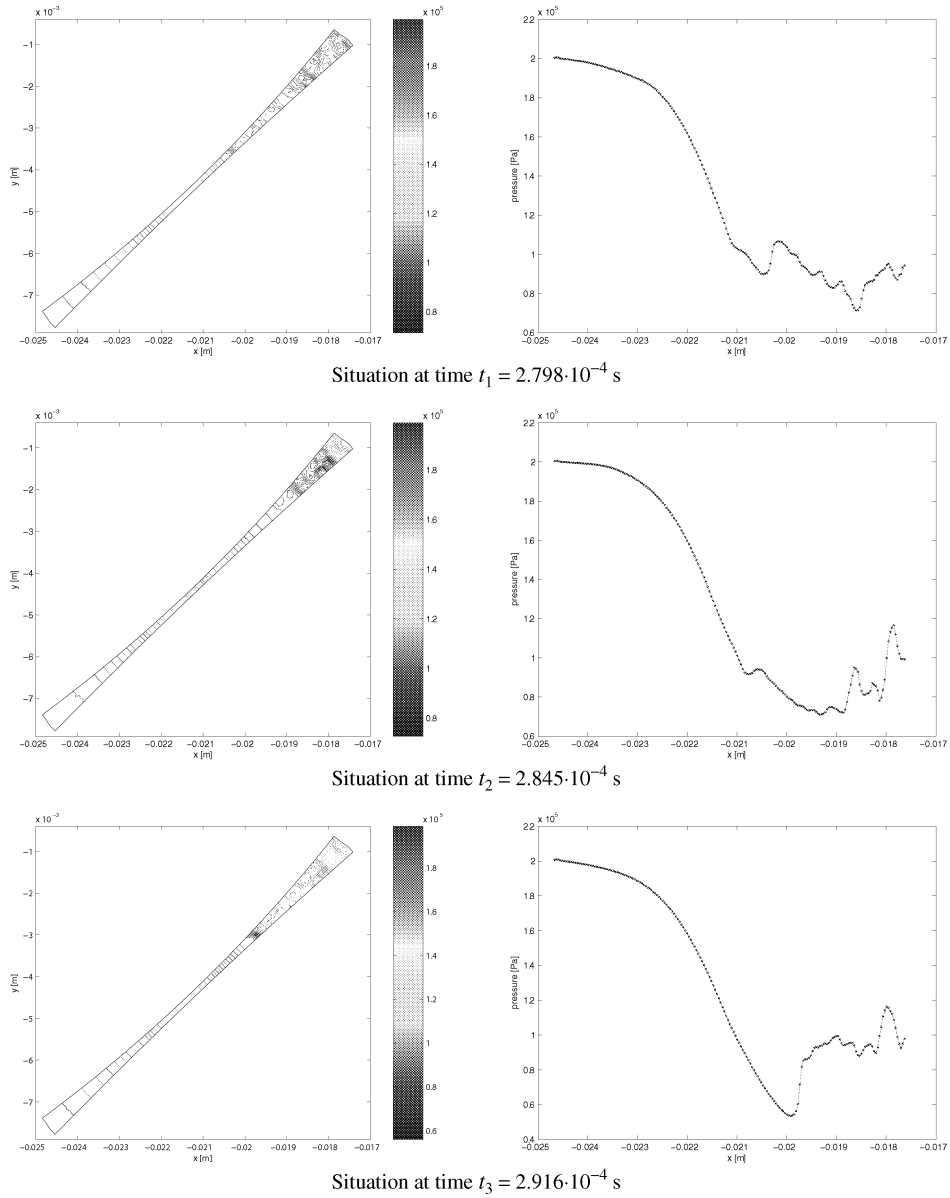

Fig.10: Isolines of the static pressure in [Pa] (left) and the static pressure distributions along a middle streamline (right) for the laminar flow computation

determined. The presented numerical method combined with the algebraic Baldwin-Lomax turbulence model gives satisfactory results in comparison with the non-stationary results obtained using the laminar flow computation. Further, the numerical method is able to work also on the computational grid refined near the walls without numerical oscillations.

A key non-dimensional parameter for gas microflows is the Knudsen number, which is defined as the ratio of the mean free path λ over a characteristic geometric length L. According to [3], the Knudsen number is related to the Reynolds and Mach numbers as

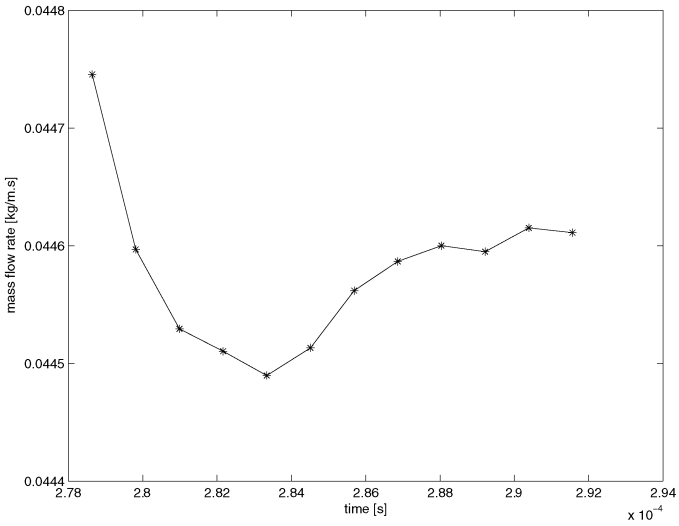

Fig.11: Mass flow rates per unit height in dependence on the time for the laminar flow computation

follows

$$Kn \equiv \frac{\lambda}{L} = \sqrt{\frac{\kappa\,\pi}{2}}\,\frac{M}{Re_\infty}\ . \tag{39}$$

All numerical computations presented in this article were performed for $Re_\infty = 3900$. This value of the reference Reynolds number leads to $Kn < 5{\cdot}10^{-4}$, i.e. the fluid can be considered as a continuum and the application of the mathematical model described by the system of the Favre-averaged Navier-Stokes equations is acceptable in our case.

This study is another step of a longer term aim to understand the fluid mechanical effects in screw-type machines.

Acknowledgement

This study has been supported by the grant GP ČR 101/03/P090 of the Grant Agency of the Czech Republic and by the research project MSM 4977751303 of the Ministry of Education, Youth and Sports of the Czech Republic to which we express our grateful thanks.

References

[1] Dvořák R.: Transonic Flows, Academia, Prague, 1986 (in Czech)
[2] Hirsch Ch.: Numerical Computation of Internal and External Flows, vol. 1, vol. 2, John Wiley & Sons, Chichester, 1990
[3] Karniadakis G., Beskok A., Aluru N.: Microflows and Nanoflows. Fundamentals and Simulation, vol. 29 of Interdisciplinary Applied Mathematics, 2005
[4] Wilcox D.C.: Turbulence Modeling for CFD, DCW Industries, La Cañada, California, 1993
[5] Baldwin B.S., Lomax H.: Thin Layer Approximation and Algebraic Model for Separated Turbulent Flows, AIAA 16th Aerospace Sciences Meeting 78-257, 1978
[6] Causon D.M.: High Resolution Finite Volume Schemes and Computational Aerodynamics, In: Nonlinear Hyperbolic Equations – Theory, Computation Methods and Applications, vol. 24 of Notes on Numerical Fluid Mechanics, Vieweg, Braunschweig, 1989, pp. 63–74

[7] Kauder K., de Araújo-Rudolph L., Sachs R.: Experimental and Numerical Investigation of the Gas Flow Using a Plane Model of Male Rotor-Housing Gap in a Screw-Type Machine, Schraubenmaschinen 8:5–16, Dortmund, 2000
[8] Kauder K., Stratmann D.: Numerische Strömungsuntersuchung der Gasspaltströmung im Hauptrotor-Gehäusespalt in Schraubenmaschinen, Schraubenmaschinen 10:49–62, Dortmund, 2002
[9] Prins J., Infante-Ferreira C.A.: Selected Basic Theory of Gas Leakage, In: Proceedings of the IMechE Conference on Compressors and Their Systems, London, 2003, pp. 521–530
[10] Švígler J., Vimmr J.: Mathematical Model of the Work Space of the Screw Machine, In: CD-ROM Proceedings of the Fifth World Congress on Computational Mechanics, Vienna, 2002
[11] Vimmr J.: Introduction to the Mathematical Modelling of Turbulent Compressible Fluid Flow, Zeszyty naukowe Katedry Mechaniki Stosowanej 21:207–212, Gliwice, 2003
[12] Vimmr J.: A Treatise on Numerical Computation of Non-Stationary Laminar Compressible Flow, In: Proceedings of the 19th Conference Computational Mechanics 2003, Hrad Nečtiny, University of West Bohemia in Pilsen, pp. 483–494
[13] Vimmr J., Švígler J.: Analysis of the Compressible Viscous Fluid Flow Through the Gap Caused by the Incorrect Contact of Screw Surfaces, In: CD-ROM Proceedings of the 10th Conference Engineering Mechanics 2004, Svratka, Institute of Thermomechanics, Academy of Sciences of the Czech Republic in Prague (in Czech)
[14] Vimmr J.: Turbulent Compressible Fluid Flow Computation in a Male Rotor-Housing Gap of Screw Compressors, Journal Proc. Appl. Math. Mech. 5:567–568, 2005
[15] Vimmr J.: Computation of a Leakage Flow in a Male Rotor-Housing Gap of Screw Compressors, In: CD-ROM Proceedings of the 16th International Symposium on Transport Phenomena, Prague, 2005
[16] Příhoda J.: Algebraic Turbulence Models and Their Application to the Solution of Averaged Navier-Stokes Equations, Research Report Z-1153/90, Institute of Thermomechanics, Academy of Sciences of the Czech Republic in Prague, 1990 (in Czech)

Received in editor's office: January 6, 2006
Approved for publishing: July 11, 2007

Note: The paper is an extended version of the contribution presented at the national conference with international participation *Engineering Mechanics 2005, Svratka, 2005.*